Ice Shape Analysis of an eVTOL Propeller in Forward Flight at the NASA Glenn Icing Research Tunnel

Paul H. von Hardenberg

Curtis A. Flack

NASA Glenn Research Center

David L. Rigby

HX5 LLC

AIAA AVIATION FORUM

July 29th – August 2nd, 2024

Background

PROBLEM While icing engineering tools and methods for means of compliance are fairly mature for existing legacy aircraft, there are no accepted icing engineering tools specifically developed and rigorously tested for AAM class vehicles.

OBJECTIVE Develop experimental and computational icing simulation capabilities for eVTOL vehicles.

APPROACH
- Acquire **experimental ice shapes** on non-proprietary propeller/rotor geometries for code validation and development.
- Establish **best practices** and **scaling methodologies** for conducting icing tests on rotating geometries.
- Acquire **experimental shedding data** to support development of ice shedding prediction capabilities.

ACCOMPLISHMENTS
- Successfully completed two test entries of a generic eVTOL propeller in the Icing Research Tunnel in 2023 and 2024.
- Acquired ice shapes, propeller performance degradation, and high-speed images of shedding events.

This presentation and corresponding paper provides an analysis of the ice shape data acquired during the 2023 test only.

NASA Tiltwing Concept Vehicle (cruise configuration)

AAM Propeller Test Stand Installed in Icing Research Tunnel (IRT)

Test Article and Instrumentation

MOTOR FEATURES

- Power: 34 kW (cont.), 60 kW (peak)
- Torque: 52 Nm (cont.), 100 Nm (peak)

TEST STAND FEATURES

- Adjustable axis of rotation for non-axial flow
- 6-axis load cell for torque and thrust measurements

MEASUREMENT CAPABILITIES

- 3D ice shape documentation
- Ice mass measurements
- High speed imaging for capturing ice shedding events
- Light strobing for real-time ice growth monitoring
- Torque and thrust measurements
- Motor current and voltage measurements

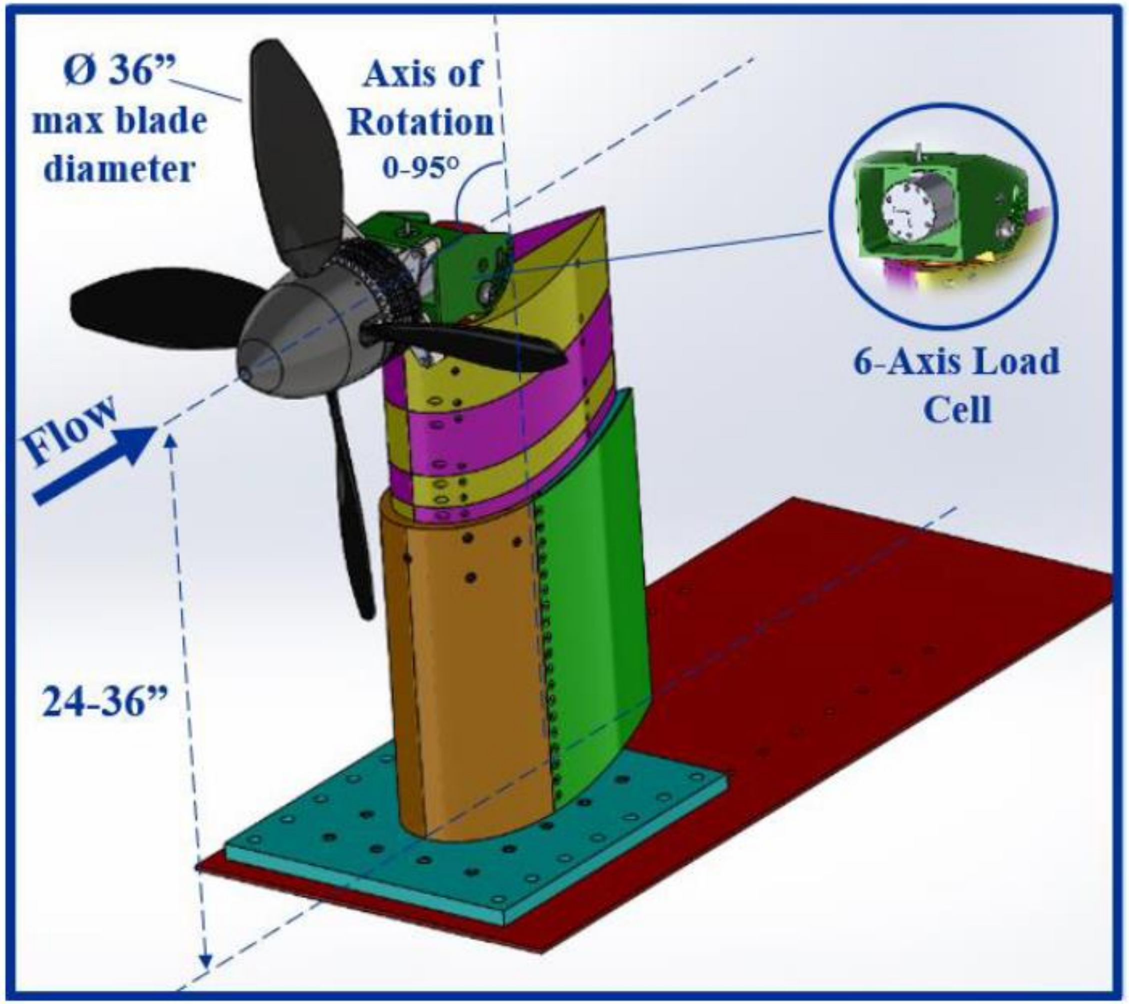

AAM Propeller Test Stand

Propeller Geometry

PROPELLER SPECIFICATIONS

- Three propellers of diameters 24, 28, and 36 inches.
- Twist and chord distributions inspired by the NASA Computationally Optimized Proprotor (COPR)*.
- NACA 0012 airfoil
- Geometrically scaled from a radial location of r/R = 0.40 and outward.
- Spinner **not** scaled with propeller size.

Diameter = Ø24”

Ø28”

Ø36”

Chord Distributions

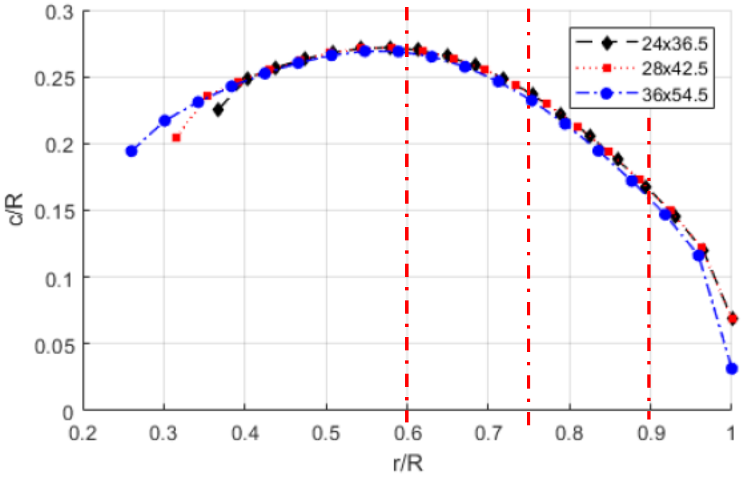

Twist Distributions

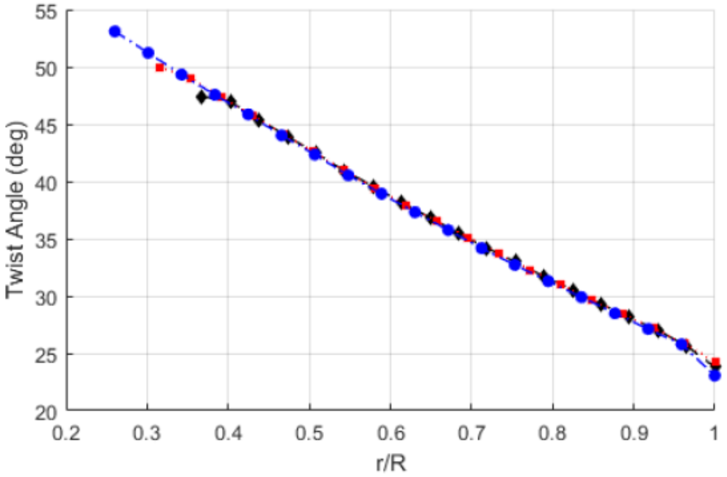

*Zawodny et al., NASA TM 20220015637, NASA Langley Research Center, 2023

Test Conditions

OPERATING CONDITIONS

Blade Diameters (in)	Tunnel Speeds (knots)	Helical Tip Speeds (Mach)	Advance Ratios
24, 28, 36	87 - 130	0.20 - 0.31	2.3 – 2.7

CLOUD CONDITIONS

MVD (μm)	LWC (g/m³)	Freestream Total Temp. (˚C)
15, 30, 80	0.55, 0.65, 1.20	-3 to -15

NOTE:

- Propeller in axial flow configuration
- Constant RPM for duration of spray
- 28” propeller accounted for 39 of the 45 total test runs

Ice Shape Repeatability

	Target Operating and Cloud Conditions								Similarity Parameters (calculated at $r/R = 0.75$)				Ice Mass	
Run	V_∞ knots	$t_{\infty,0}$ °C	δ μm	LWC g/m³	τ min	RPM rev/min	D in	J	n_0^*	A_c	β_0	We_L 10^6	Blade g	Spinner g
RA3683	87	-15.0	15	0.55	3.0	1516	28	2.49	2.37	2.59	0.88	0.15	9.0	10.6
RA3687	"	"	"	"	"	"	"	"	"	"	"	"	8.5	10.3
RA3714	"	"	"	"	"	"	"	"	"	"	"	"	9.8	10.8

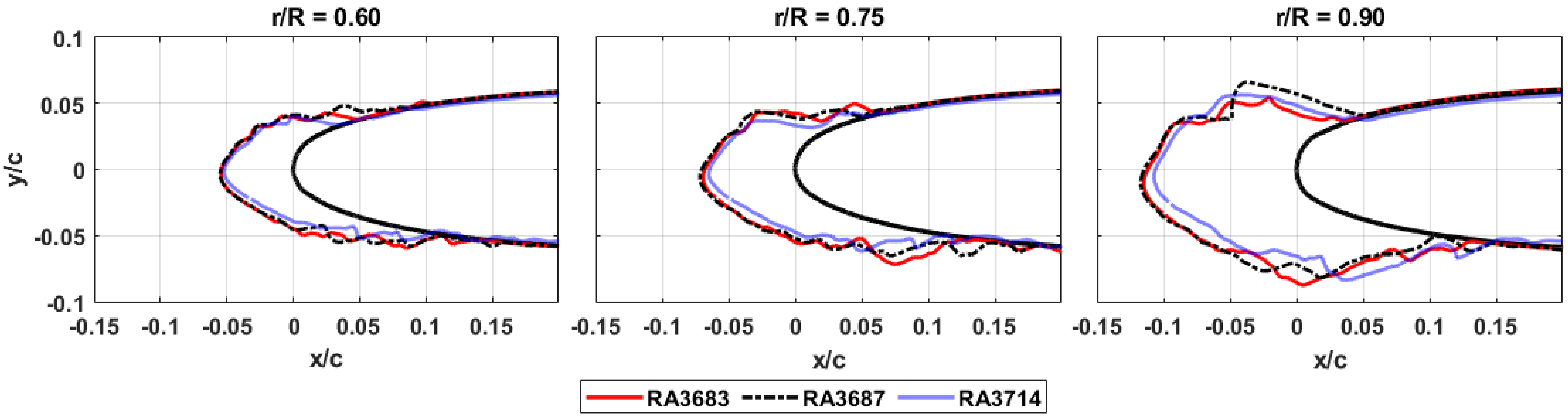

Effect of Freestream Total Air Temperature

	Target Operating and Cloud Conditions								Similarity Parameters (calculated at $r/R = 0.75$)				Ice Mass	
Run	V_∞ knots	$t_{\infty,0}$ °C	δ µm	LWC g/m^3	τ min	RPM rev/min	D in	J	n_0^*	A_c	β_0	We_L 10^6	Blade g	Spinner g
RA3701	87	-3.0	15	0.55	3.0	1516	28	2.49	0.51	2.59	0.88	0.15	7.0	8.4
RA3702	"	-6.0	"	"	"	"	"	"	1.01	"	"	"	8.3	9.3
RA3705	"	-7.5	"	"	"	"	"	"	1.26	"	"	"	9.7	10.1

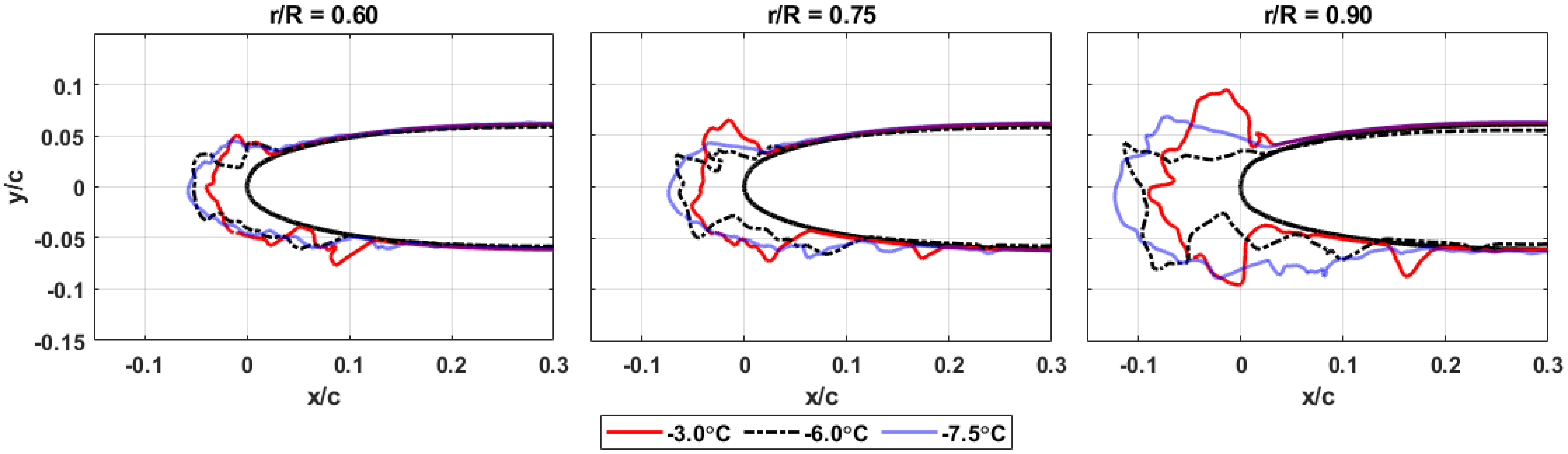

Effect of Temperature (cont.)

Run	Target Operating and Cloud Conditions								Similarity Parameters (calculated at $r/R = 0.75$)				Ice Mass	
	V_∞ knots	$t_{\infty,0}$ °C	δ µm	LWC g/m^3	τ min	RPM rev/min	D in	J	n_0^*	A_c	β_0	We_L 10^6	Blade g	Spinner g
RA3705	87	-7.5	15	0.55	3.0	1516	28	2.49	1.26	2.59	0.88	0.15	9.7	10.1
RA3703	"	-9.0	"	"	"	"	"	"	1.49	"	"	"	8.7	9.8
RA3704	"	-12.0	"	"	"	"	"	"	1.94	"	"	"	9.1	9.8
RA3683	"	-15.0	"	"	"	"	"	"	2.37	"	"	"	9.0	10.6

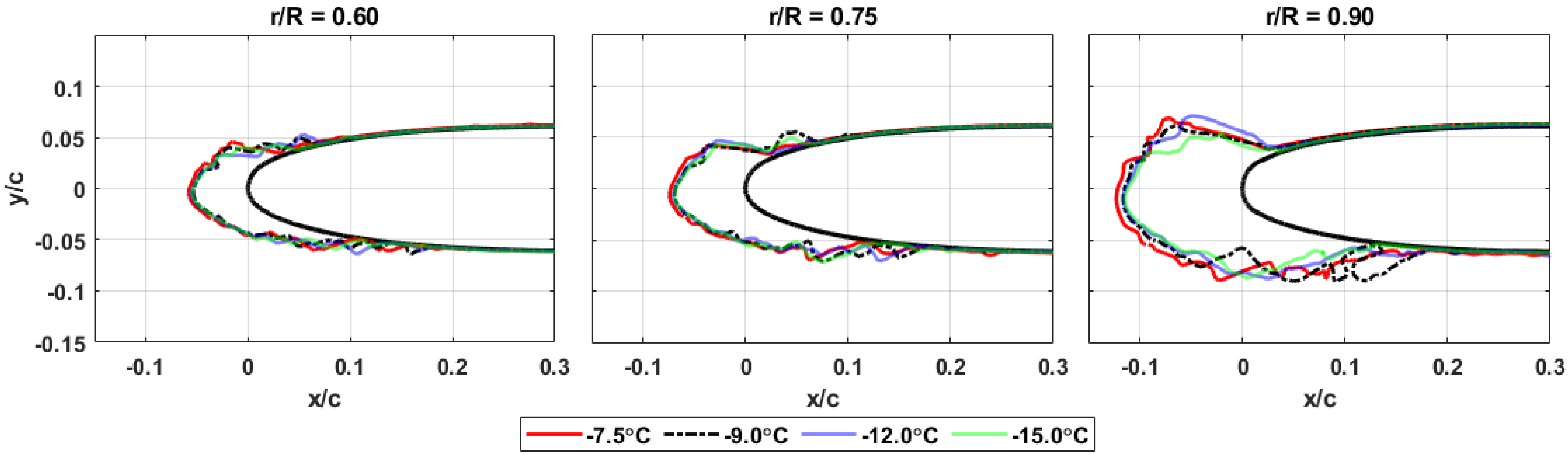

Effect of Temperature (cont.)

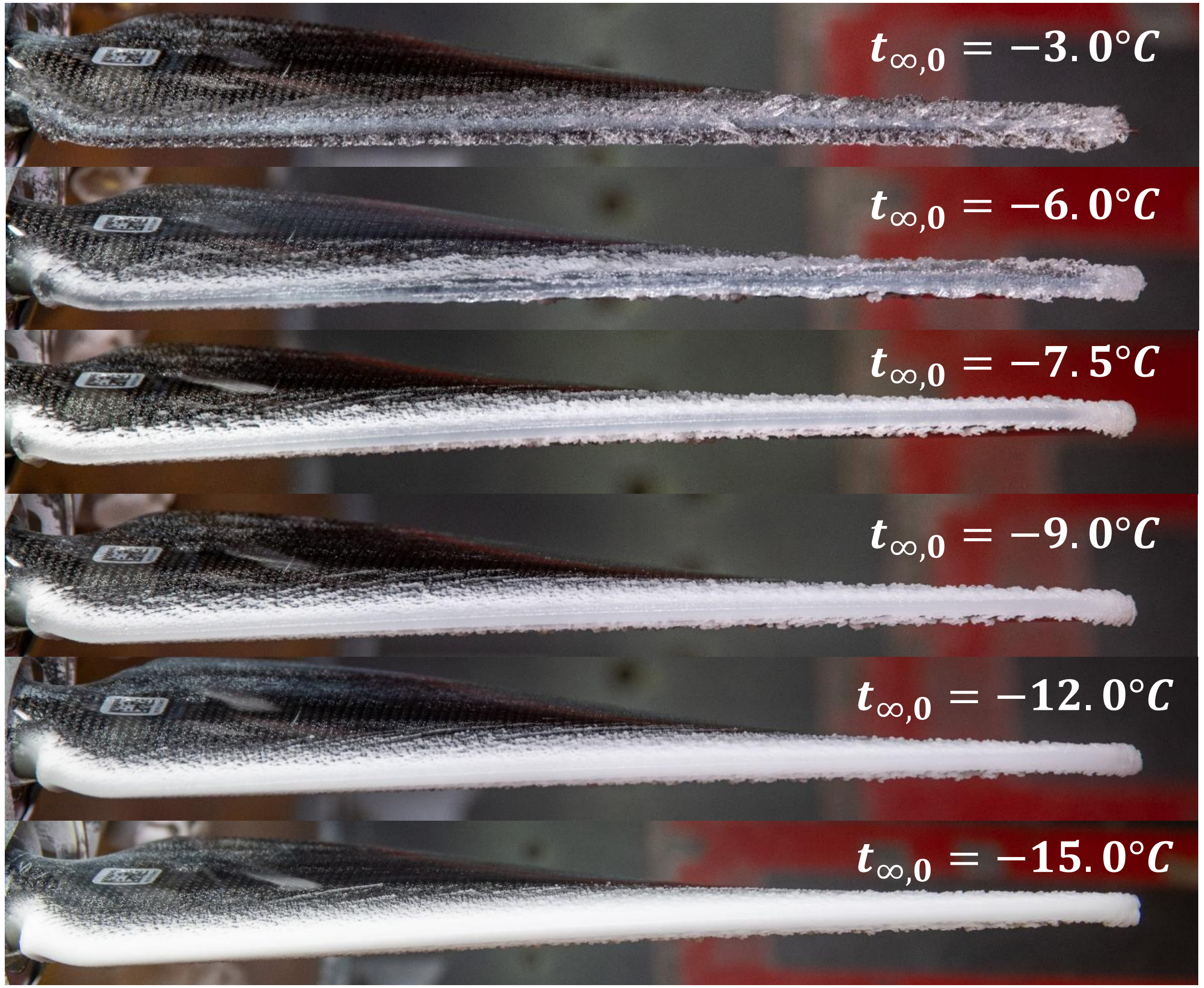

$n_0^* = 0.51$

$n_0^* = 1.01$

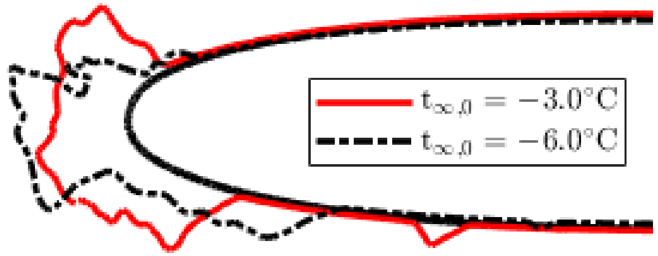

$n_0^* = 1.26$

$n_0^* = 1.49$

$n_0^* = 1.94$

$n_0^* = 2.37$

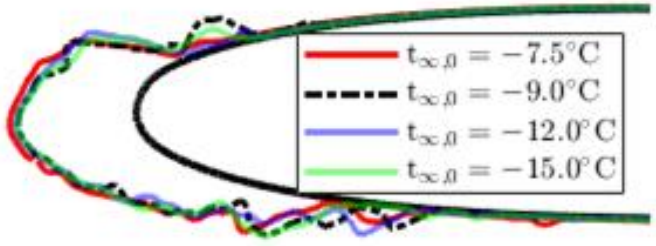

Effect of Icing Time (n_0 = 1.0)

Run	Target Operating and Cloud Conditions								Similarity Parameters (calculated at $r/R = 0.75$)				Ice Mass	
	V_∞ knots	$t_{\infty,0}$ °C	δ µm	LWC g/m^3	τ min	RPM rev/min	D in	J	n_0^*	A_c	β_0	We_L 10^6	Blade g	Spinner g
RA3693	87	-15.0	15	0.55	1.5	1516	28	2.49	2.37	1.30	0.88	0.15	4.2	5.1
RA3683	"	"	"	"	3.0	"	"	"	"	2.59	"	"	9.0	10.6
RA3695	"	"	"	"	4.5	"	"	"	"	3.89	"	"	10.7*	15.9
RA3711	"	"	"	"	6.0	"	"	"	"	5.18	"	"	21.0	21.5

*Ice mass affected due to shedding

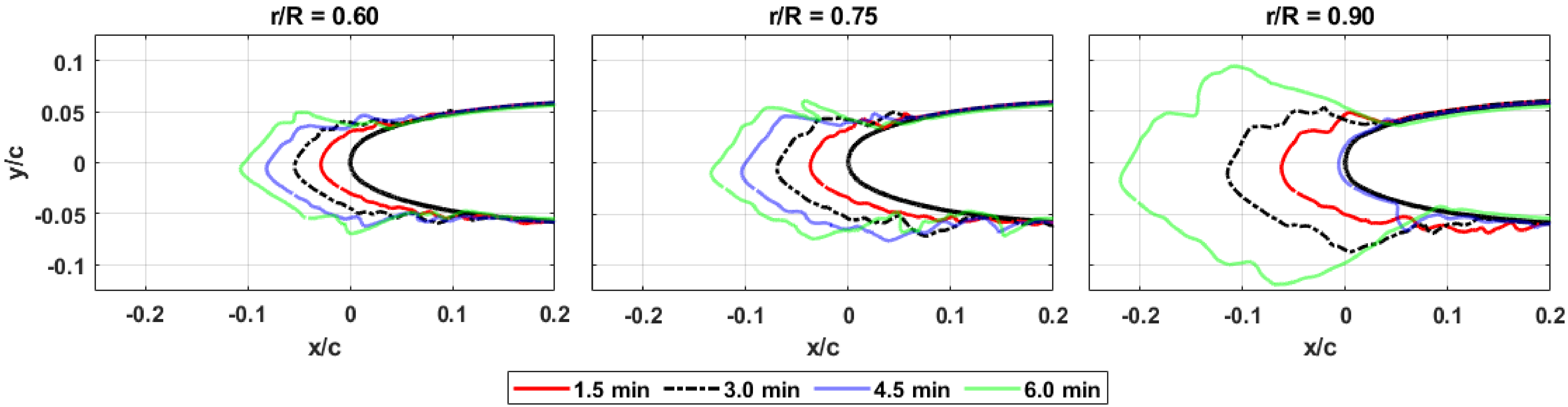

Effect of Icing Time ($n_0 < 1.0$)

Run	Target Operating and Cloud Conditions								Similarity Parameters (calculated at $r/R = 0.75$)				Ice Mass	
	V_∞ knots	$t_{\infty,0}$ °C	δ µm	LWC g/m^3	τ min	RPM rev/min	D in	J	n_0^*	A_c	β_0	We_L 10^6	Blade g	Spinner g
RA3690	87	-6.0	15	1.20	1.4	1516	28	2.49	0.51	2.64	0.88	0.15	9.0	12.8
RA3691	"	"	"	"	2.1	"	"	"	"	3.96	"	"	18.7	23.3
RA3692	"	"	"	"	2.8	"	"	"	"	5.28	"	"	28.0	32.3

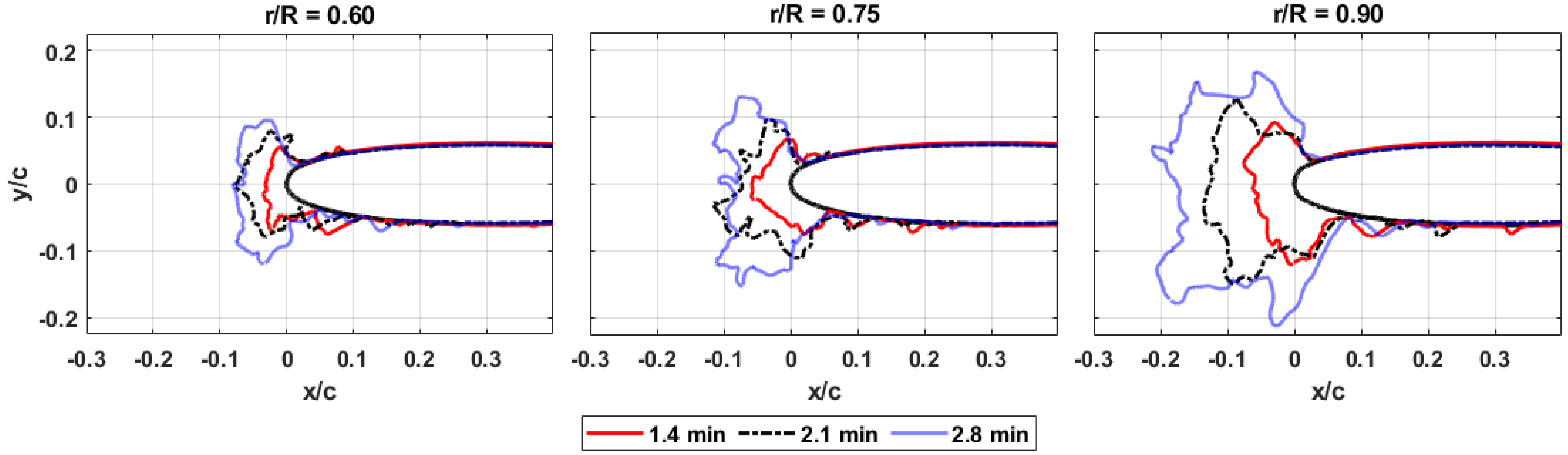

Effect of Icing Time

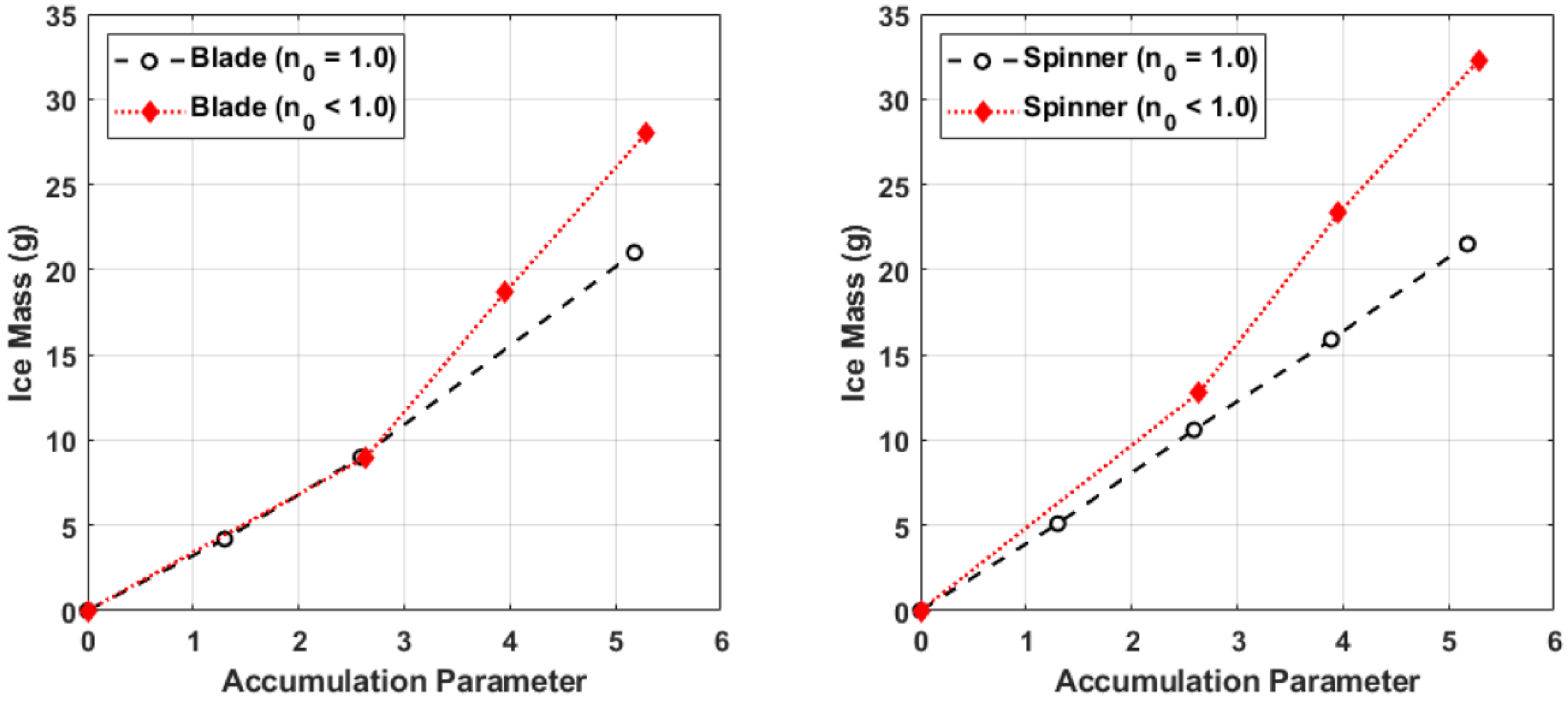

(a) Blade Ice Mass (b) Spinner Ice Mass

Effect of MVD

	Target Operating and Cloud Conditions								Similarity Parameters (calculated at $r/R = 0.75$)				Ice Mass	
Run	V_∞ knots	$t_{\infty,0}$ °C	δ µm	LWC g/m^3	τ min	RPM rev/min	D in	J	n_0^*	A_c	β_0	We_L 10^6	Blade g	Spinner g
RA3683	87	-15.0	15	0.55	3.0	1516	28	2.49	2.37	2.59	0.88	0.15	9.0	10.6
RA3713	"	"	30	0.65	2.5	"	"	"	1.90	2.55	0.95	"	11.1	28.7
RA3686	"	"	80	0.55	3.0	"	"	"	2.13	2.59	0.99	"	11.9	45.3

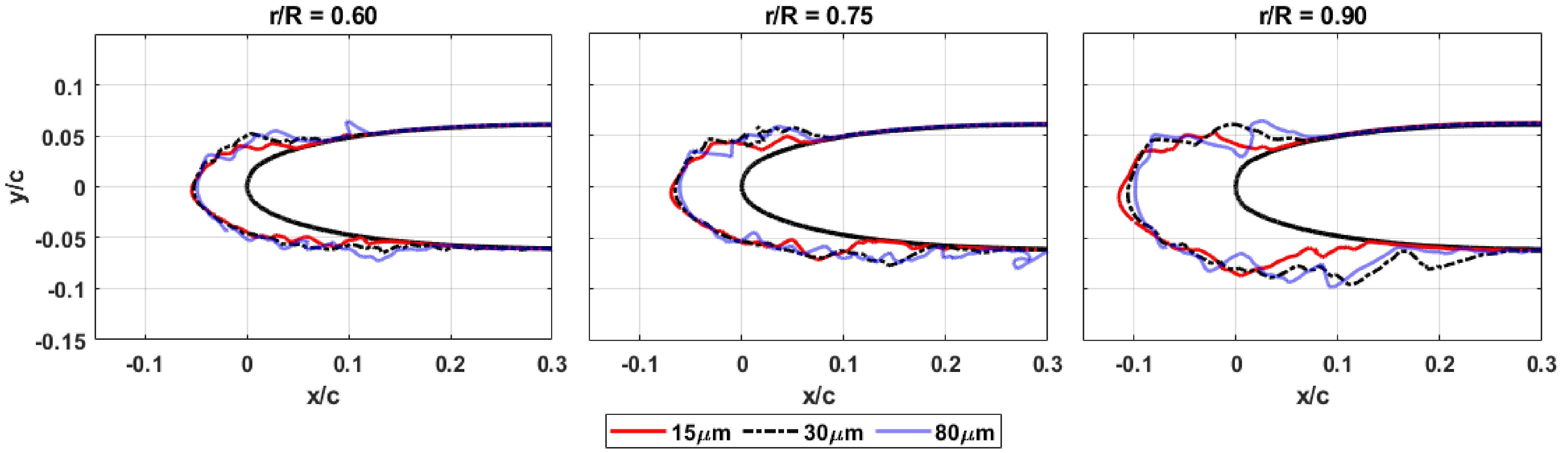

Effect of MVD cont.

15 MVD

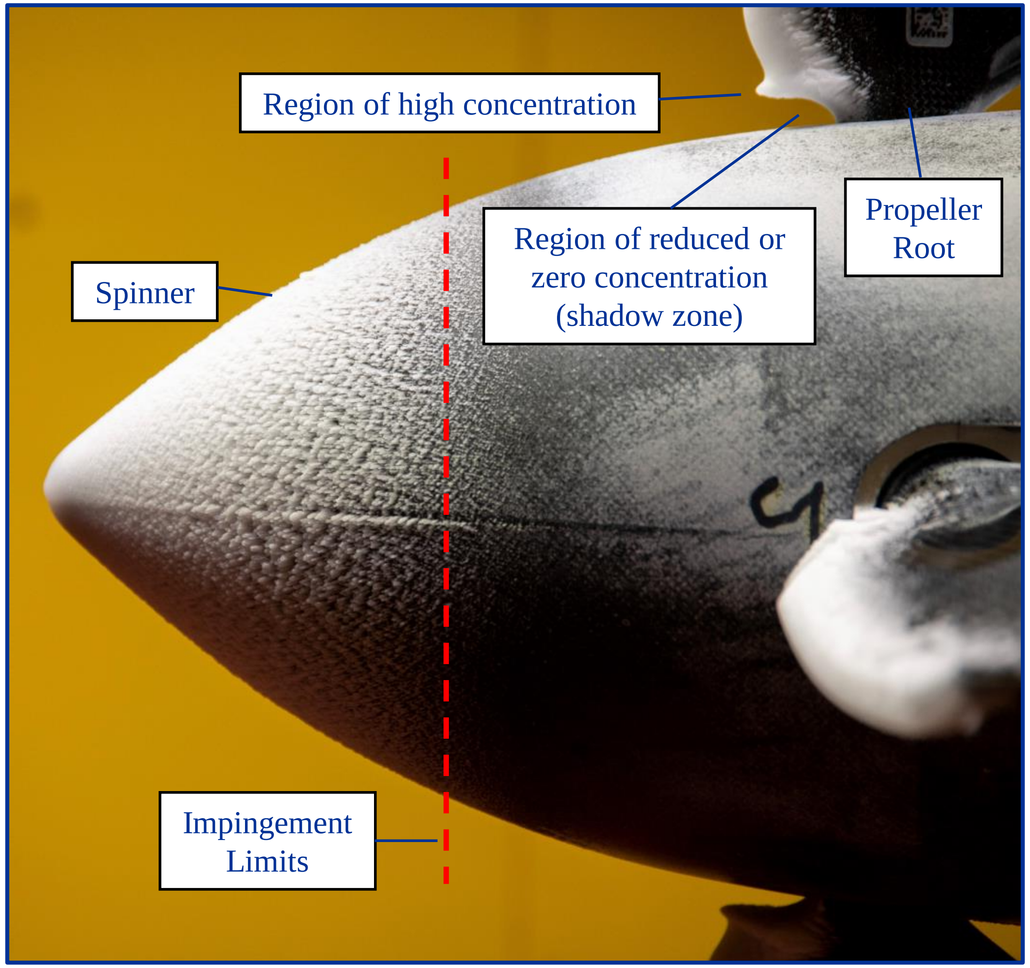

80 MVD

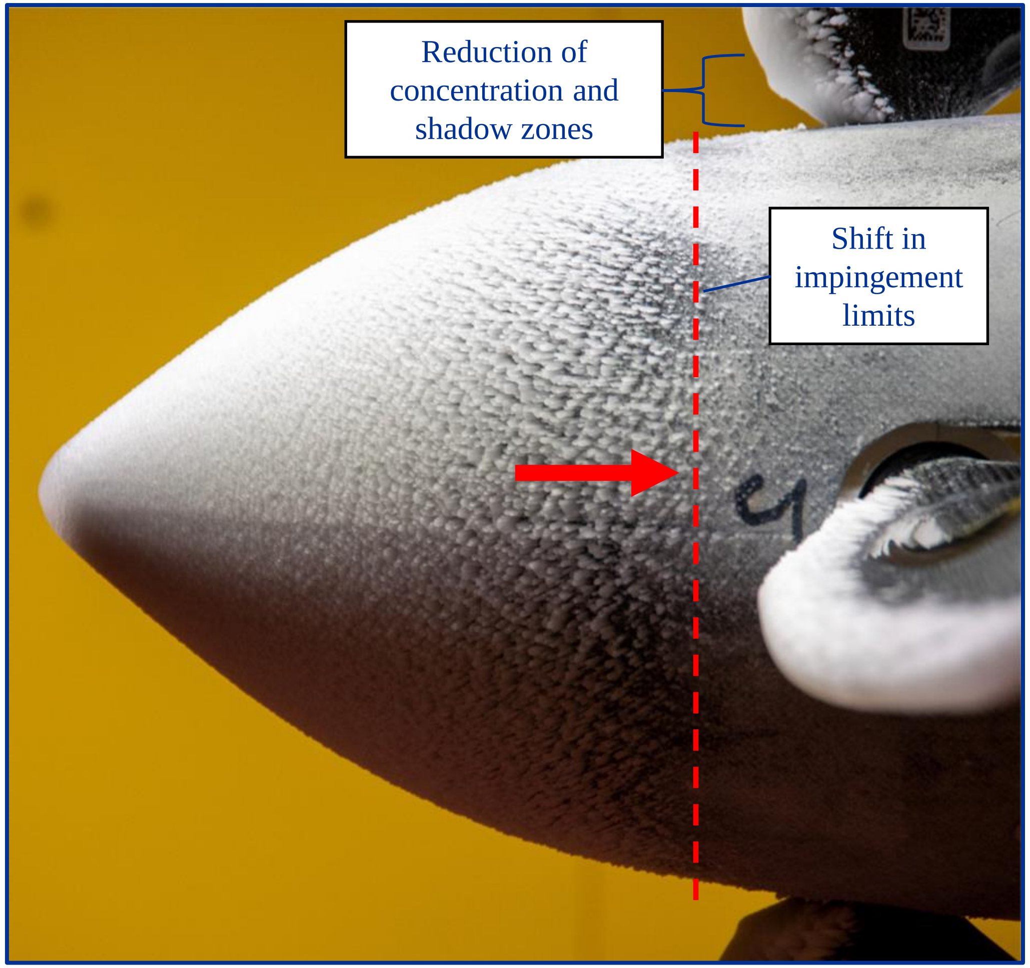

Effect of MVD cont.

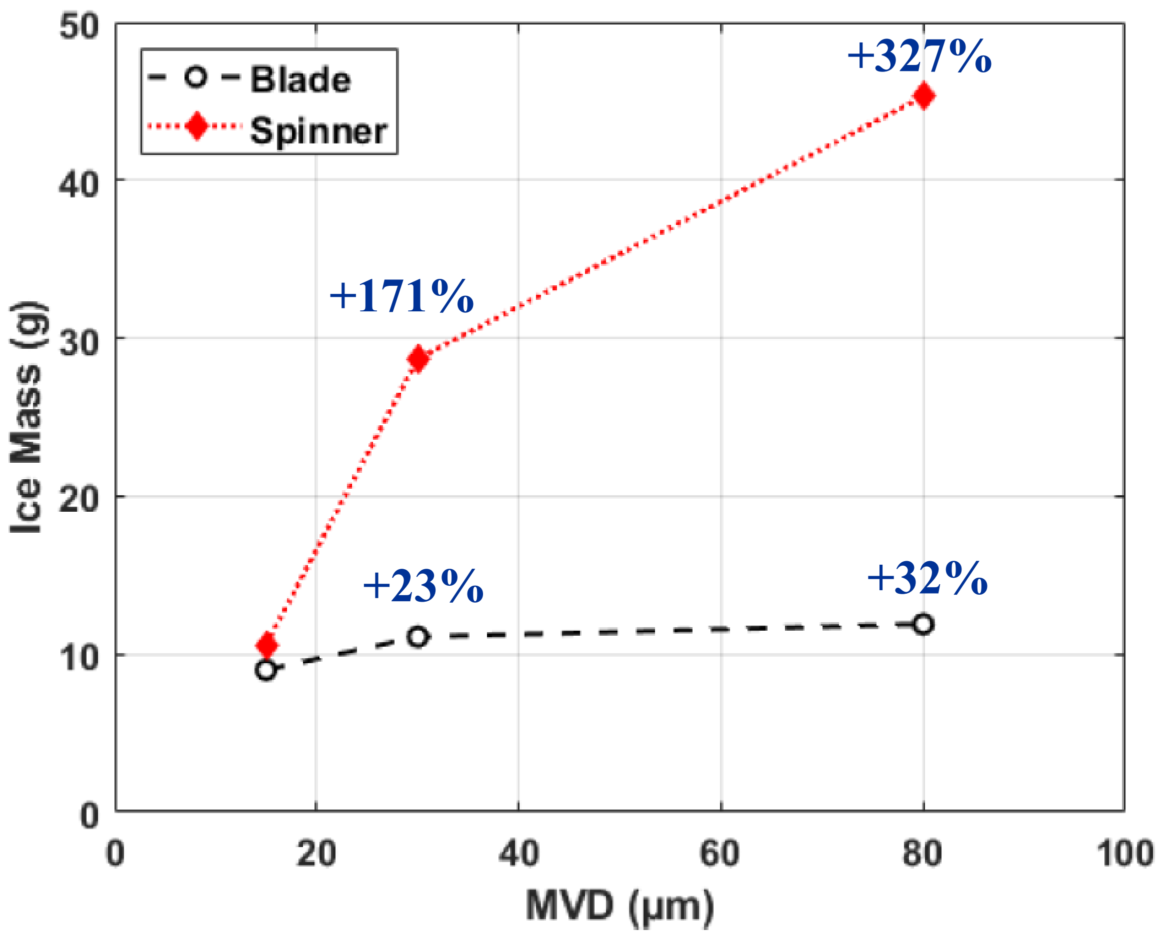

Scaling for LWC ($n_0 < 1.0$)

	Target Operating and Cloud Conditions								Similarity Parameters (calculated at $r/R = 0.75$)				Ice Mass	
Run	V_∞ knots	$t_{\infty,0}$ °C	δ µm	LWC g/m^3	τ min	RPM rev/min	D in	J	n_0^*	A_c	β_0	We_L 10^6	Blade g	Spinner g
RA3701	87	-3.0	15	0.55	3.0	1516	28	2.49	0.51	2.59	0.88	0.15	7.0	8.4
RA3690	"	-6.0	"	1.20	1.4	"	"	"	"	2.64	"	"	9.0	12.8

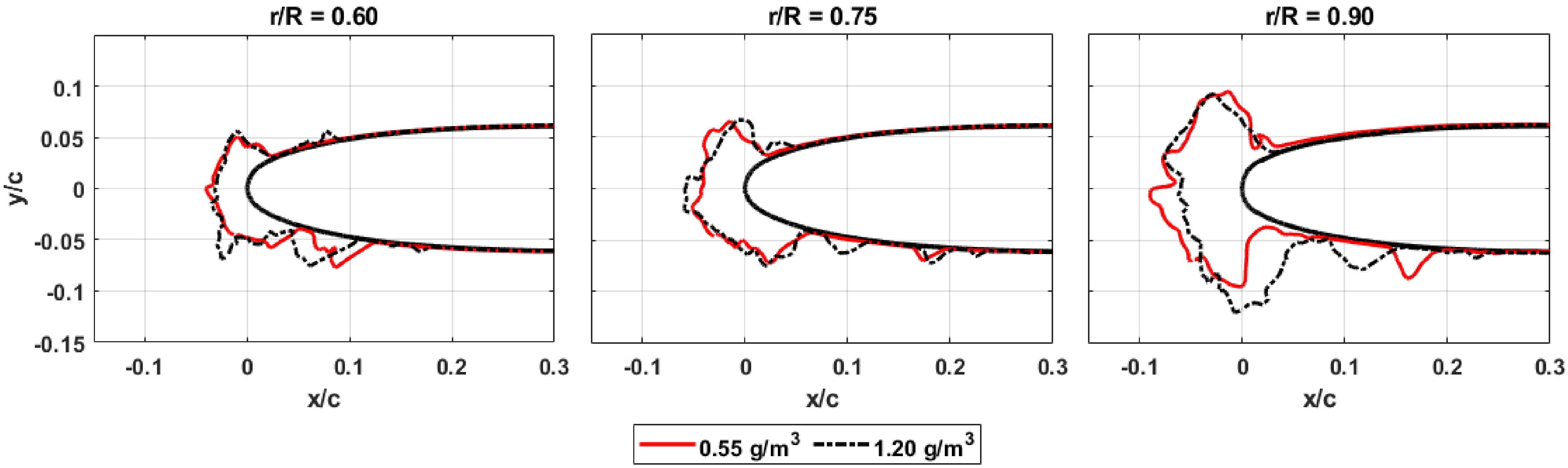

Scaling for Propeller Size

Run	Target Operating and Cloud Conditions								Similarity Parameters (calculated at $r/R = 0.75$)				Ice Mass	
	V_∞ knots	$t_{\infty,0}$ °C	δ µm	LWC g/m^3	τ min	RPM rev/min	D in	J	n_0^*	A_c	β_0	We_L 10^6	Blade g	Spinner g
RA3717	95	-12.0	15	0.55	3.4	1928	24	2.49	1.95	3.76	0.90	0.15	8.3	14.0
RA3698	"	"	"	"	4.0	1657	28	2.49	1.84	3.78	0.89	0.18	15.1	17.3
RA3681	"	"	"	"	5.0	1300	36	2.47	1.67	3.67	0.86	0.23	28.3	20.8

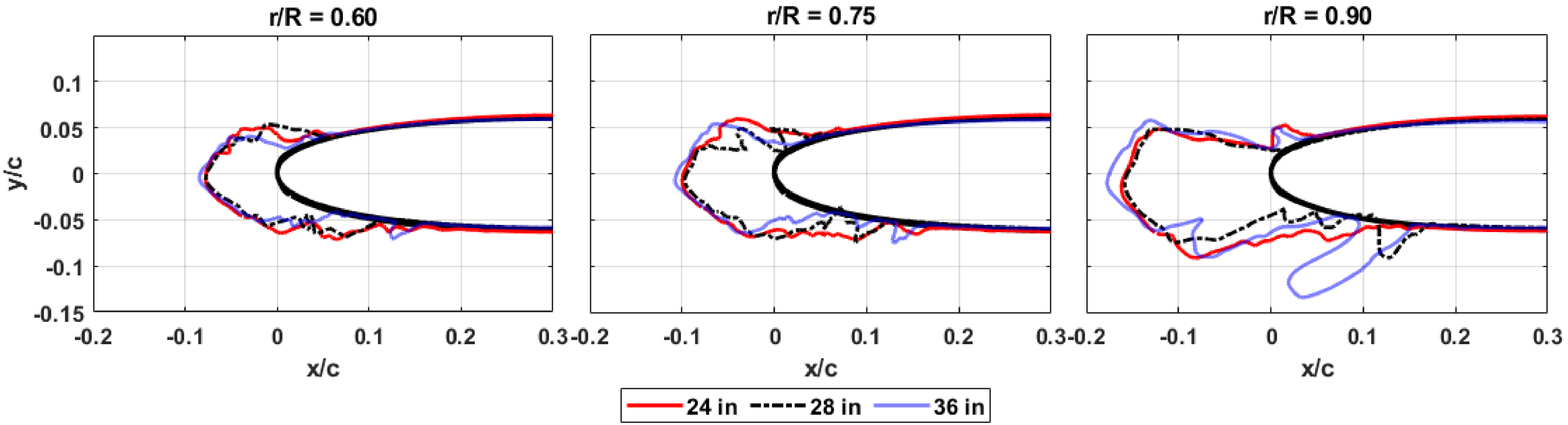

Summary and Conclusion

- Ice shapes were generated on a non-proprietary eVTOL propeller in an axial flow (forward flight) configuration in the Icing Research Tunnel.
- Ice shapes were reviewed for their repeatability, correctness of trends, and sensitivity to parameter variations.
- Icing similarity parameters were calculated at discrete radial locations
  - Qualitatively useful and followed predicted trends.
  - Appeared to overestimate freezing fraction.
- Fixed wing scaling methods were applied to the propeller with promising results.
  - More data is needed over a wider range of conditions and propellers sizes to provide confidence in the scaling method.

Acknowledgments

This work was funded by the NASA **R**evolutionary **V**ertical **L**ift **T**echnology (**RVLT**) project.

Special thanks to the NASA Glenn Icing Branch and the IRT personnel for their invaluable support throughout this effort.

Contact Information

Paul H. von Hardenberg

NASA Glenn Research Center

paul.h.vonhardenberg@nasa.gov

Backup Slides

Calculation of Icing Similarity Parameters

Key Icing Similarity Parameters

Parameter	Variable	Description
Freezing Fraction	n	Fraction of water flux entering a control volume that freezes within the control volume.
Collection Efficiency	β	Fraction of the freestream droplet concentration that impinges on a surface.
Accumulation Parameter	A_c	Theoretical maximum leading edge ice thickness normalized by the airfoil leading edge nose diameter of curvature.
Weber's Number	We_L	Ratio of the inertial forces acting on a drop to its surface tension.

- Icing similarity parameters were calculated at stagnation for discrete radial locations along the blade.
- **NOTE:** Freezing Potential (n^*) = Freezing Fraction (n) with no upper limit.

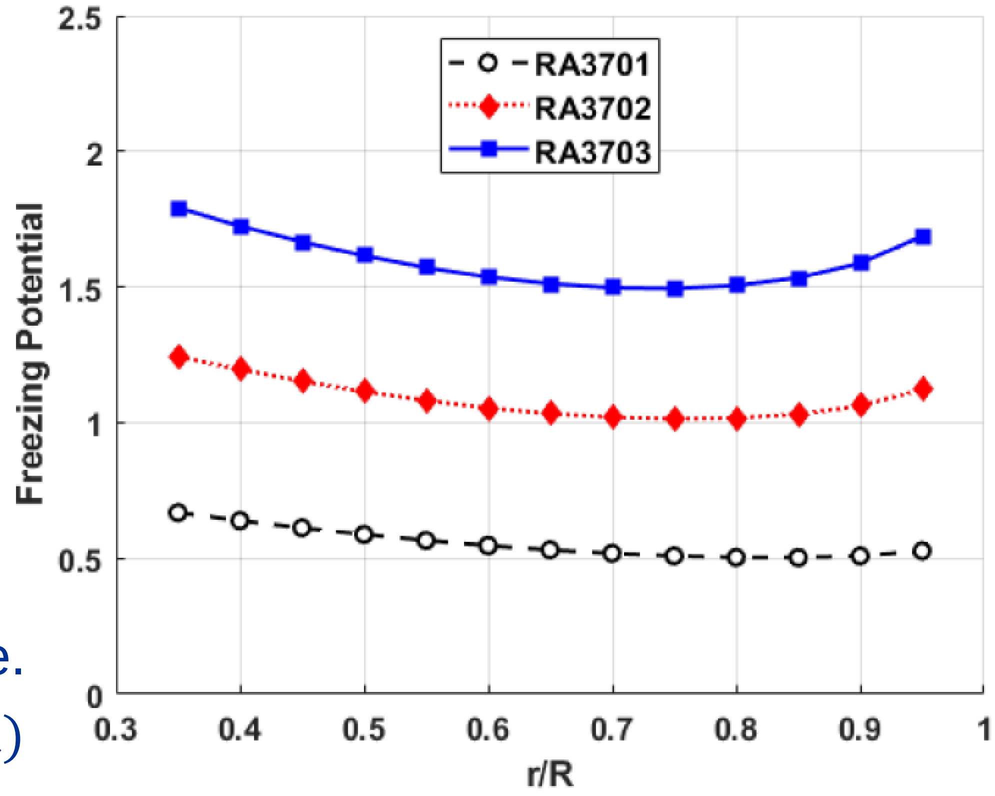

Example Freezing Potential vs Span Distributions

Calculation of Icing Similarity Parameters

- Icing scaling methods for unprotected fixed airfoils have been well established [1, 2].
- There remains to be an accepted and rigorously tested icing scaling method for rotating airfoils.
- Application of fixed-wing icing scaling methods to rotating airfoils offers a good starting point.

They key icing similarity parameters (Table 1) can be estimated by substituting the **effective velocity**, $\boldsymbol{V_{eff}}$, for the **freestream velocity**, $\boldsymbol{V_{\infty}}$, during the derivations of those parameters.

For this study, the effects of propeller induction were ignored such that:

$$\boldsymbol{V_{eff} \approx \sqrt{(V_{\infty})^2 + (\omega r)^2}}$$

Table 1: Description of Important Icing Similarity Parameters

Parameter	Variable	Description
Freezing Fraction	n	Fraction of water flux entering a control volume that freezes within the control volume.
Collection Efficiency	β	Fraction of the freestream droplet concentration that impinges on a surface.
Accumulation Parameter	A_c	Theoretical maximum leading edge ice thickness normalized by the airfoil leading edge nose diameter of curvature.
Weber's Number	We_L	Ratio of the inertial forces acting on a drop to its surface tension.

- Freezing fraction has a theoretical upper limit of n = 1.0
- However, calculation of n can sometimes produce values greater than 1.0
- The unbounded value of n will be presented which will hereinafter be referred to as the **Freezing Potential,** $\boldsymbol{n^*}$

Effect of MVD cont.

15 MVD | **30 MVD** | **80 MVD**

(high pressure side)